Available online at www.sciencedirect.com
SCIENCE DIRECT®
Biochemical and Biophysical Research Communications 311 (2003) 193–201
BBRC
www.elsevier.com/locate/ybbrc

Crystal structure of *Salmonella typhimurium* 2-methylisocitrate lyase (PrpB) and its complex with pyruvate and Mg^{2+}

Dhirendra K. Simanshu,[a] P.S. Satheshkumar,[b] H.S. Savithri,[b] and M.R.N. Murthy[a,*]

[a] *Molecular Biophysics Unit, Indian Institute of Science, Bangalore, India*
[b] *Department of Biochemistry, Indian Institute of Science, Bangalore, India*

Received 23 September 2003

Abstract

Propionate metabolism in *Salmonella typhimurium* occurs via 2-methylcitric acid cycle. The last step of this cycle, the cleavage of 2-methylisocitrate to succinate and pyruvate, is catalysed by 2-methylisocitrate lyase (PrpB). Here we report the X-ray crystal structure of the native and the pyruvate/Mg^{2+} bound PrpB from *S. typhimurium*, determined at 2.1 and 2.3 Å, respectively. The structure closely resembles that of the *Escherichia coli* enzyme. Unlike the *E. coli* PrpB, Mg^{2+} could not be located in the native *Salmonella* PrpB. Only in pyruvate bound PrpB structure, Mg^{2+} was found coordinated with pyruvate. Binding of pyruvate to PrpB seems to induce movement of the Mg^{2+} by 2.5 Å from its position found in *E. coli* native PrpB. In both the native enzyme and pyruvate/Mg^{2+} bound forms, the active site loop is completely disordered. Examination of the pocket in which pyruvate and glyoxalate bind to 2-methylisocitrate lyase and isocitrate lyase, respectively, reveals plausible rationale for different substrate specificities of these two enzymes. Structural similarities in substrate and metal atom binding site as well as presence of similar residues in the active site suggest possible similarities in the reaction mechanism.

Keywords: *Salmonella typhimurium*; 2-Methylisocitrate lyase; Helix swapping; Propionate metabolism; Isocitrate lyase; Crystal structure

Acetate and propionate are the two most abundant low molecular mass carbon compounds in soil. Many aerobic microorganisms, bacteria, and fungi as well as some anaerobes have the ability to utilize propionate as their sole carbon and energy source. Extensive analyses of propionic acid metabolism in various organisms have elucidated at least seven different pathways [1]. All known degradation pathways of propionate start with the activation of the fatty acid as propionyl-CoA. In most vertebrates, propionate degradation is carried out by α-carboxylation of propionyl-CoA to (*S*)-methylmalonyl-CoA, which racemizes to the (*R*)-enantiomer. The latter rearranges in a vitamin B_{12}-dependent reaction to succinyl-CoA. Plants, insects, and microorganisms make use of a number of alternate pathways for propionate breakdown.

In the recent past, the catabolism of propionate in prokaryotes has been extensively investigated. It has been demonstrated that propionate is metabolized to pyruvate via 2-methylcitric acid cycle in *Salmonella enterica* [2] as well as in *Escherichia coli* [3]. This pathway was initially postulated by studies with mutant strains of *Candida lipolytica*, in which accumulation of either methylcitrate or 2-methylisocitrate was observed during growth on odd-chain fatty acids, which were degraded via propionyl-CoA [4]. Earlier to these studies, 2-methylcitric acid cycle was thought to occur only in yeasts and molds.

In *S. enterica* serovar Typhimurium (herein after referred to as *Salmonella typhimurium*), a locus on the chromosome essential for growth on propionate, was identified [5]. Genetic and molecular characterization of this locus identified four enzymes and a sigma-54-dependent transcriptional activator organized as a *prpRBCDE* operon [6]. Oxidation of propionate starts with the enzyme prpE, a propionyl-CoA synthetase, which forms propionyl-CoA from propionate and acetyl-CoA. prpC, a 2-methylcitrate synthase, forms 2-methylcitrate by the condensation of propionyl-CoA

* Corresponding author. Fax: +91-80-360-0535.
E-mail address: mrn@mbu.iisc.ernet.in (M.R.N. Murthy).

0006-291X/$ - see front matter © 2003 Elsevier Inc. All rights reserved.
doi:10.1016/j.bbrc.2003.09.193

and oxaloacetate. The 2-methylcitrate thus formed is converted to 2-methylisocitrate in two enzymatic steps involving prpD, a methylcitrate dehydratase, and one of the two aconitases present [7]. prpB, a 2-methylisocitrate lyase, catalyses the last step of this cycle, which involves the cleavage of 2-methylisocitrate to succinate and pyruvate as shown in Fig. 1. Succinate is further oxidized to oxaloacetate for condensation with propionyl-CoA forming methylcitrate and completing the cycle. The end product of the pathway, pyruvate, can be used further for energy metabolism and synthesis of biomass.

When cultured in the presence of glucose, propionate and other short chain fatty acids (SCFAs) have the additional property of inhibiting cell growth, which has made them useful as preservatives in the food industry. The growth inhibiting effect of propionate, in the presence of glucose, may be due to the accumulation of propionyl-CoA which leads to competition among other housekeeping genes dealing with CoA-esters as substrate or product [8]. Sensitivity against propionate has been found to increase drastically when 2-methylcitrate pathway is blocked in *Salmonella*, suggesting that intermediates of this pathway may have a more profound negative impact on cell growth compared to propionate [9]. Therefore, structure determination of the enzymes involved in this pathway will give information on specific inhibition of these enzymes, which can lead to methods for reducing the amount of propionate required for food preservation [10].

Oxidation of propionate via 2-methylcitric acid cycle resembles the part of the glyoxylate cycle in which acetate is oxidized to glyoxylate. Isocitrate lyase, involved in glyoxalate cycle, is related to 2-methylisocitrate lyase with respect to catalytic reaction. In this paper, we report the X-ray crystal structure of the native as well as pyruvate and Mg^{2+} bound 2-methylisocitrate lyase (EC 4.1.3.30) from *S. typhimurium* IFO 12529. The structure was determined using the *E. coli* PrpB enzyme as the starting phasing model [10]. As in isocitrate lyases, the polypeptide is made of a $(\alpha\beta)_8$ barrel. The results reveal the differences between *Salmonella* and *E. coli* enzymes and provide further insights into the structure–function relationships. Differences in the structure of isocitrate lyase and 2-methylisocitrate lyase and residues involved in the binding site of pyruvate/glyoxalate in these two enzymes are also discussed.

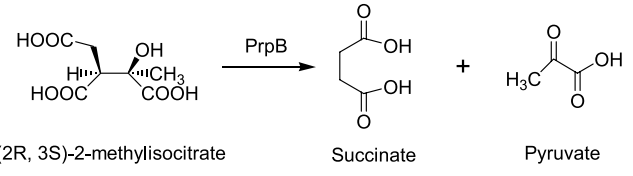

Fig. 1. Reaction catalysed by 2-methylisocitrate lyase (PrpB) leading to the cleavage of 2-methylisocitrate into succinate and pyruvate.

Materials and methods

Crystallization. S. enterica serovar Typhimurium strain IFO 12529 was a gift from Prof. Toru Nagasawa, Okayama University, Japan. Recombinant PrpB was expressed, purified, and crystallized using different conditions as previously described [11]. In brief, prpB gene was PCR amplified from *S. typhimurium* genomic DNA and expressed in the host strain *E. coli* BL21 (DE3). Soluble fraction of the expressed protein was purified using Ni^{2+}–NTA superflow (Qiagen). Purity of the protein was monitored by SDS–PAGE. About 35 mg of the protein could be obtained from 1 L culture. The sequence of the *prpB* gene was determined by nucleotide sequencing and confirmed by comparing it with the *prpB* gene of *S. typhimurium* LT2.

Crystallization was carried out with the hanging drop as well as the sitting drop vapour diffusion methods. Crystals used for X-ray diffraction data collection were obtained at 291 K from solutions containing 0.1 M imidazole, pH 6.5, and 1.0 M sodium acetate trihydrate for the native protein. For co-crystallization experiments, PrpB was incubated overnight with 50 mM of pyruvic acid. Crystals of pyruvate bound PrpB appeared in 2 M NaCl, 10% PEG6000. On the basis of the proposed reaction mechanism in isocitrate lyases [12], in PrpB, pyruvate is expected to bind first followed by binding of succinate. Therefore, crystals obtained in the presence of pyruvate were soaked in 50 mM succinate for 3 h before data collection.

Data collection. Complete three-dimensional X-ray diffraction data were collected for the native PrpB and the ligand bound PrpB extending to a resolution of 2.1 and 2.3 Å, respectively, at 100 K. Prior to flash cooling, glycerol was added, up to 20% by volume, to the crystallization drop. Both the datasets were collected at 100 K using a MAR research image plate system (diameter 345 mm) mounted on a Rigaku RU200 rotating anode X-ray generator equipped with a 200μ focal cup. The X-ray beam was focussed using Osmic mirrors. Datasets for both the crystals were processed using the programs *DENZO* and *SCALEPACK* [13]. Data quality program was used to obtain data statistics [14].

Structure determination and refinement. Initial attempts to determine the structure of PrpB using *Mytilus edulis* phosphoenolpyruvate mutase (PDB code 1PYM) were not successful [15]. With the view of determining the structure by multiple isomorphous replacement, a mercurial derivative was produced by soaking the crystals in solutions containing 5 mM *para*-chloro-mercuribenzene sulphonic acid (PCMBS). Analysis of the difference Patterson maps revealed four major sites. However, an electron density map based on this single derivative was not interpretable. Around this time, the structure of 2-methylisocitrate lyase (PrpB) from *E. coli* was published [10]. The orientation and position of the tetrameric 2-methylisocitrate lyase molecule in the $P2_12_12_1$ asymmetric unit could easily be determined using the *E. coli* PrpB enzyme (PDB code 1MUM) [10] as the starting model in the Molecular Replacement method program AMoRe [16]. A PrpB model corresponding to the molecular replacement solution was subjected to refinement using CNS1.1 [17]. The data between 20.0 and 2.1 Å were used for the refinement, setting aside 5% of the data for cross-validation. After initial rigid body and positional refinement, sigma weighted $2F_o - F_c$ and $F_o - F_c$ maps were calculated and visualized using the interactive model-building program O [18]. Model building was alternated with iterations of rigid body, positional, and individual temperature factor refinements. This was followed by identification of potential sites of solvent molecules, first by automatic water-picking algorithm of CNS1.1 [17] and then manually on the basis of $2F_o - F_c$ and $F_o - F_c$ maps. Positional and *B*-value parameters of all the atoms, including protein and water, were further refined. The structure of ligand bound PrpB was solved using native PrpB as the starting model. This was followed by structural refinement using a protocol similar to the one used for the native structure.

Root-mean-square deviations from ideal geometries for bond lengths and bond angles were calculated with CNS 1.1 [17]. The ste-

reochemical quality of the final model was assessed by the program PROCHECK [19]. Average *B* factors for protein atoms, water molecules, and ligands were calculated using BAVERAGE program of CCP4 suite [20]. Atomic models were superposed using the program ALIGN [21].

Results and discussion

The structures of the native and the pyruvate/Mg^{2+} bound 2-methylisocitrate lyase (PrpB) have been determined to a resolution of 2.1 and 2.3 Å, respectively. In both the cases, the asymmetric unit contains a tetramer, the active oligomeric state, with 222 symmetry. These subunits are designated as A, B, C, and D in the following discussions.

Overall structure of native PrpB

The standard procedure of molecular replacement using AMoRe [16] was used to solve the structure using *E. coli* PrpB as the starting model [10]. For the molecular replacement solution, the correlation was 53.0% and the *R* factor was 38.7% for the reflections in the resolution range of 15–3.5 Å. The final model was refined at 2.1 Å to an *R* factor of 20.5% and R_{free} of 23.2%. The data collection and refinement statistics of native PrpB is given in Table 1. In the final map, the electron density is of good quality for most of the model. However, significant and unambiguous density was not found in three different places: the N terminal 3–4 residues; the active site loop between fourth β-strand and sixth α-helix (residues

Table 1
Data collection and refinement statistics

Data set	Native PrpB	Pyruvate/Mg^{2+} bound PrpB
(A) Data collection		
Space group	$P2_12_12_1$	$P2_12_12_1$
Unit cell parameters (Å)		
a (Å)	62.812	62.953
b (Å)	99.086	99.679
c (Å)	201.571	202.396
No. of monomers per asymmetric unit	4	4
Resolution range (Å)	20.0–2.1	20.0–2.3
No. of observations	391,895	273,290
No. of unique reflections	70,807	53,974
$I/\sigma(I)$	15.5 (5.2)	17.0 (5.6)
Completeness in %	95.4 (97.2)	94.0 (99.5)
Multiplicity	5.5	5.1
R_{merge}[a] (%)	6.1 (42.2)	6.4 (28.8)
$R_{measure}$[a] (%)	6.7 (46.3)	7.2 (32.0)
R_{sym}[b] (%)	6.1 (42.3)	6.4 (28.9)
(B) Refinement		
R-factor (%)	20.5 (24.3)	20.0 (22.9)
R_{free} (%)	23.2 (27.6)	25.2 (29.3)
No. of atoms		
Protein atoms	8220	8196
Solvent atoms	565	553
Metal atoms	0	4
Ligand	0	24
RMS deviation from ideal values		
Bond length (Å)	0.006	0.006
Bond angle (deg.)	1.10	1.10
Residues in Ramachandran plot (%)		
Most allowed region	92.3	91.4
Allowed region	7.3	8.2
Generously allowed region	0.3	0.2
Disallowed region	0.1	0.2
Average *B* factors (Å^2)		
Overall	38.8	40.7
Protein	38.67	40.74
Water	40.178	39.9
Mg^{2+}	0	41.337
Pyruvic acid	0	38.604

Values in parentheses correspond to the highest resolution shell.

[a] $R_{merge} = 100 \times \sum_h \sum_i^{n_h} |\hat{I}_h - I_{h,i}| / \sum_h \sum_i^{n_h} I_{h,i}$ and $R_{measure} = 100 \times 100 \times \sum_h [n_h/(n_h-1)]^{1/2} \sum_i^{n_h} |\hat{I} - I_{h,i}| / \sum_h \sum_i^{n_h} I_{h,i}$ where $\hat{I}_h = (1/n_h) \sum_i^{n_h} I_{h,i}$ and n_h is the multiplicity [14].

[b] $R_{sym} = 100 \times \sum |\langle I \rangle - I| / \sum \langle I \rangle$ where $\langle I \rangle$ is the mean intensity of the reflections.

118–129), and the last 6–13 C-terminal residues in different subunits. The structure has acceptable stereochemistry with 92.3% of all residues in the most favoured region of the Ramachandran plot calculated with the program PROCHECK [19]. Only Asp 87 within each subunit falls at a position corresponding to the generously allowed/disallowed region of the Ramachandran plot. This residue is directly involved in binding Mg^{2+}.

Like all members of the isocitrate lyase family, which have been biochemically characterized so far [12,22–24], PrpB forms a homotetramer [25]. In the crystal structure, contacts across one of the 2-folds (AB dimer) are very extensive in comparison with other 2-folds (AC and AD dimers) giving predominantly a dimer of a dimer appearance to the tetramer (Fig. 2A). The monomeric structure consists of an $(\alpha\beta)_8$ barrel motif, reminiscent

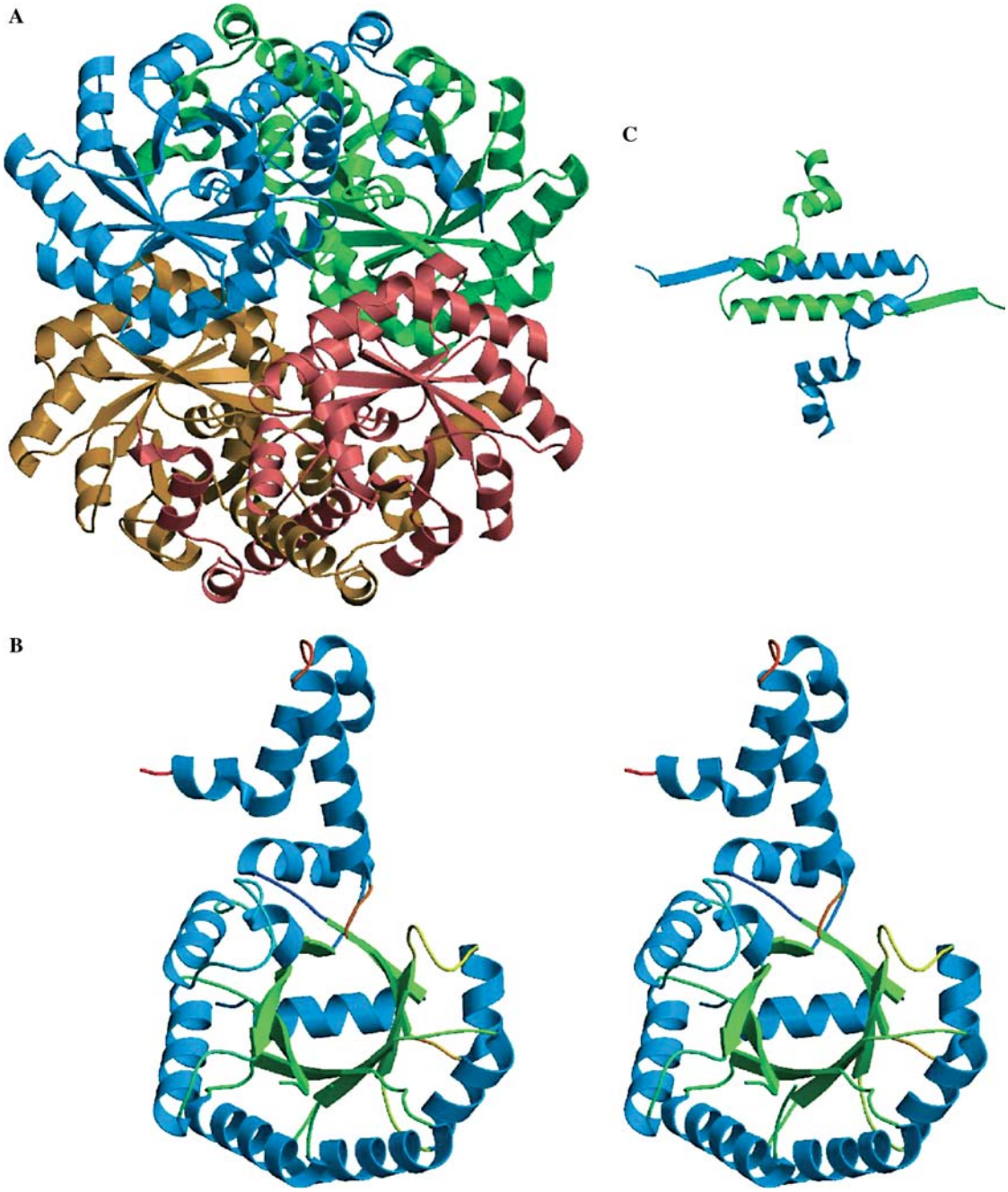

Fig. 2. The structure of 2-methylisocitrate lyase (PrpB). (A) The quaternary structure of homotetrameric 2-methylisocitrate lyase (dimer of dimers), with each subunit coloured differently. The four subunits are related by 222 symmetry. (B) Stereo view of monomer. The α-helices are shown in skyblue and the β-strands are shown in green. The carboxy terminal eighth helix of the monomer is not part of the $(\alpha\beta)_8$ barrel of the same subunit. Therefore, the overall fold consists of $(\beta/\alpha)_7\beta$. (C) Illustration of the "helix swapping" interaction between A/B and C/D subunits in 2-methylisocitrate lyase (PrpB). The figures were generated using MOLSCRIPT [28] and rendered using Raster3D [29].

of TIM barrels. The inner strands are longer when compared to the canonical triose phosphate isomerase strands. As in *E. coli* PrpB and other isocitrate lyases, the carboxy-terminal eighth helix of the monomer A is not part of the $(\alpha\beta)_8$ barrel of the same subunit. It protrudes away from the A subunit and fills a similar cavity in the $(\alpha\beta)$ barrel of the B subunit. Thus, the overall fold consists of $(\beta/\alpha)_7\beta$ as shown in Fig. 2B. Exchange of the eighth helix between symmetry related subunits has been called " helix swapping." This exchange leads to the formation of a partial "knot" like structure such that the four subunits cannot be separated from each other without conformational changes in a loop region between the two helical segments of the swapped region (Fig. 2C). Helix swapping is thought to provide a mechanism for oligomeric assembly concomitant with folding.

Structural comparison with E. coli PrpB

Because of high sequence identity (89%) between PrpB from *S. typhimurium* and *E. coli*, we expected almost identical polypeptide folds. However, some differences were indeed observed. Further, these differences were found in and around the active site, in particular the electron density of active site loop and mode of binding of Mg^{2+}.

In *E. coli* PrpB as well as other isocitrate lyases, the active site loop between fourth β-strand and sixth α-helix of the $(\alpha\beta)_8$ barrel moves from an "open" state in the ligand free enzyme to a "closed" state upon ligand binding. The open conformation of this loop in the *E. coli* PrpB enzyme is distinct from the corresponding conformation in isocitrate lyases reflecting the conformational variability of this segment [10]. The loop is found to be completely disordered in *Salmonella* PrpB.

In the enzymes of isocitrate lyase family, the catalysis is strictly dependent on Mg^{2+}. Accordingly, a Mg^{2+} is observed within the active site of *E. coli* PrpB [10] and all isocitrate lyase crystal structures determined so far, regardless of whether Mg^{2+} has been added for crystallization or not [12,22,23]. But in the present case, where Mg^{2+} was not added during the purification and crystallization experiments, electron density for the Mg^{2+} could not be located in the native PrpB. However, there is some evidence of bound Mg^{2+} in the A and B subunits. In C subunit, electron density for Asp 87 is very poor whereas in D subunit no electron density was found for Asp 87 side chain. The low occupancy of Mg^{2+} probably has led to a degree of order in Asp 87 in A and B subunits. Despite the absence of Mg^{2+} in the present case, Asp 87, which is directly coordinated to Mg^{2+} in the *E. coli* native PrpB, is present in an unfavourable region of the Ramachandran plot. Unlike *E. coli* PrpB, Pro 18 was found in the *cis*-configuration in all the four subunits.

Structural comparison with bacterial isocitrate lyase

2-Methylisocitrate lyase from *S. typhimurium* has a molecular mass of approximately 32 kDa per subunit, which is 35% lower than the molecular mass of bacterial isocitrate lyase that is approximately 48 kDa per subunit. The PrpB protein is therefore the smallest of the isocitrate lyase family and seems to have all essential amino acids conserved. The **KKCGH** sequence at the catalytic site of isocitrate lyase from *E. coli* is conserved in all other known isocitrate lyases. In contrast, PrpB from *S. typhimurium* and *E. coli*, the deduced 2-methylisocitrate lyase from *Saccharomyces cerevisiae* [26], carboxyphospho*enol*pyruvate phosphonomutase from *Streptomyces hygroscopicus* [27], and five proteobacterial homologues of PrpB contain the slightly modified sequence **KRCGH** in the catalytic site [24]. Comparison of structures of *S. typhimurium* PrpB and *E. coli* isocitrate lyase shows a number of insertions, present only in the latter enzyme (Fig. 3). In both the enzymes the N terminal end is shielded from the solvent by an α-helix. In *E. coli* isocitrate lyase, two more α-helices, which are not present in PrpB, precede this helix. The eighth helix present at the C-terminal, which is involved in helix swapping, is prolonged by 15–20 residues in bacterial isocitrate lyases compared to PrpB. Insertion of 25–30 residues between sixth β-strand (PrpB) and seventh

Fig. 3. Structural superposition of 2-methylisocitrate lyase (shown in sky blue on web; dark shade in print) from *Salmonella typhimurium* and isocitrate lyase (shown in green on web; light shade in print) from *E. coli* depicting regions conserved in PrpB, the smallest member of the isocitrate lyase family. Regions that are absent in PrpB but present in isocitrate lyase are coloured in coral on web (black in print). The figure was generated using MOLSCRIPT [28] and rendered using Raster3D [29]. (For interpretation of the references to colour in this figure legend, the reader is referred to the web version of this paper.)

α-helix (PrpB) in the case of isocitrate lyases forms an extra pair of β-strands resulting in the formation of an antiparallel β-sheet. The sixth α-helix in isocitrate lyase, corresponding to fourth α-helix of PrpB, is longer by 10–12 residues and is followed by an additional extended loop.

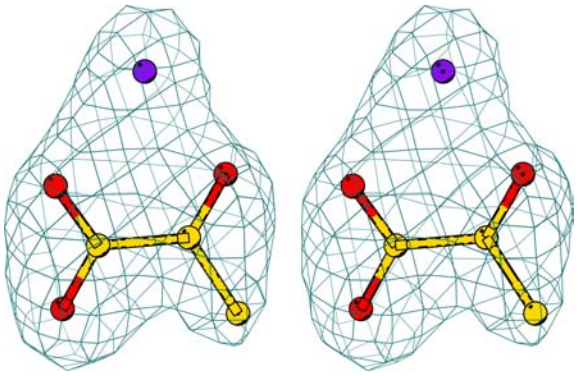

Fig. 4. Stereo view of the electron density corresponding to pyruvic acid and Mg^{2+} in the $F_o - F_c$ map. The contours are drawn at 3σ. The figure was prepared using BOBSCRIPT [30].

Overall structure of pyruvate/Mg^{2+} bound PrpB

The structure of ligand bound PrpB was solved using native PrpB as the starting model. In the final map, the electron density is of good quality for most of the protein atoms. Electron densities corresponding to pyruvate and Mg^{2+} were easily located. But no electron density was observed for succinate. Breaks in the electron density occur at equivalent regions to breaks observed in the native PrpB structure in each subunit. The final model was refined at 2.3 Å to an R factor of 20.0% and R_{free} of 25.1%. The structure shows good stereochemistry with 91.4% of all residues in the most favoured region of the Ramachandran plot calculated with the program PROCHECK [19]. The data collection and refinement statistics of pyruvate/Mg^{2+} bound PrpB is given in Table 1.

Unlike native PrpB, Mg^{2+} could be easily located in the pyruvate bound PrpB model (Fig. 4). In the $F_o - F_c$ map of pyruvate bound PrpB model, weak electron density is present near Asp 87 which seems to correspond to the Mg^{2+} position as seen in native PrpB from *E. coli* [10]. However, confident assignment was not

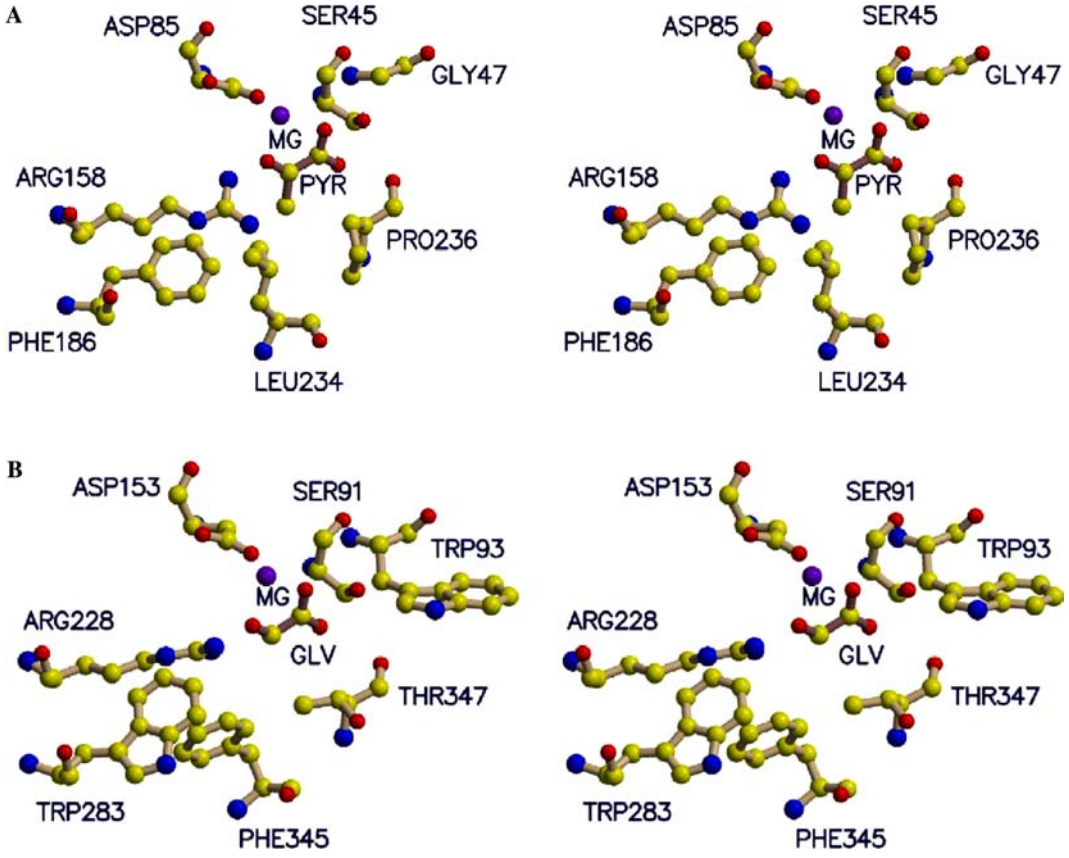

Fig. 5. Stereo view of (A) interaction of Mg^{2+} and pyruvate with *S. typhimurium* 2-methylisocitrate lyase (PrpB) and (B) interaction of Mg^{2+} and glyoxalate with isocitrate lyase from *Mycobaterium tuberculosis.* Residues Phe 186, Leu 234, and Pro 236 in PrpB and Trp 283, Phe 186, and Thr 347 in isocitrate lyase appear to provide substrate specificity for pyruvate and glyoxalate, respectively. The figures were generated using MOLSCRIPT [28] and Raster3D [29].

possible due to the very low occupancy. Binding of pyruvate seems to trigger the movement of Mg^{2+} away from Asp 87. This movement is approximately 2.5 Å towards pyruvate.

The pyruvic acid binds with the two-carboxylate groups coordinating to Mg^{2+}, which in turn interacts with two (A and C subunits) or three (B and D subunits) water molecules and with the carboxylate group of Asp 85 (Fig. 5). The Mg^{2+} ligands are arranged in octahedral geometry in B and D subunits and square bipyramidal geometry in A and C subunits. In the model, cation–ligand distances have slightly larger deviation from the target values, probably due to the presence of Mg^{2+} with partial occupancy at two different places, one close to pyruvate as in PrpB-pyruvate model and another close to Asp 87 as in *E. coli* PrpB.

In pyruvate bound PrpB model, pyruvate-protein interactions occur mainly through Ser 45 OG, Gly 47 N, and Arg 158 NH1 of the protein (Fig. 5A). These residues are conserved in isocitrate lyases, which bind glyoxalate. However in the ligand bound isocitrate lyase from *Mycobacterium tuberculosis*, glyoxalate binds to residues Ser 91 OG, Gly 92 N, Trp 93 N, and Arg 228 NH2 of the protein (Fig. 5B) [12]. Methyl group of pyruvate in the present case is placed in a hydrophobic depression formed by Phe 186, Leu 234, and Pro 236. In all known isocitrate lyases, these three residues are replaced by Trp, Phe, and Thr. Replacement of glyoxalate by pyruvate in the glyoxalate binding pocket of isocitrate lyase brings Thr347 in close contact with the methyl group of pyruvate. Therefore, it seems that the presence of these three residues, Phe 186, Leu 234, and Pro 236 in PrpB; Trp, Phe, and Thr in isocitrate lyases, provide substrate specificity for pyruvate and glyoxalate, respectively. Accordingly, sequence comparison between all known bacterial 2-methylisocitrate lyases and isocitrate lyases shows that these three residues, Phe, Leu, and Pro in case of PrpB and Trp, Phe, and Thr in case of isocitrate lyases, are strictly conserved [10].

Catalytic mechanism

All the residues thought to be involved in the catalysis of isocitrate lyase are conserved in 2-methylisocitrate lyase. Since these two enzymes catalyse similar reactions with the substrates differing in only one methyl group, 2-methylisocitrate instead of isocitrate or pyruvate instead of glyoxalate (in the reverse reaction), both the enzymes seem to follow the same reaction mechanism. Recently, site directed mutagenesis experiments on *Salmonella* PrpB have shown that Cys 123, present in 2-methylisocitrate lyase signature sequence KR**C**GH, and Asp 58 are critical to catalysis [25]. PrpB residue Cys 123 is proposed to serve as the active site base [25] and residue Asp 58 is critical for the coordination to the Mg^{2+} as seen in the *E. coli* native PrpB [10].

Sharma et al. [12] have proposed a reaction mechanism for the isocitrate lyase, deduced from an analysis of crystal structures of native and inhibitor bound forms of isocitrate lyase. In the reverse reaction catalysed by isocitrate lyase, in which glyoxalate and succinate are condensed to isocitrate, glyoxalate binds first and is followed by binding of succinate to form a ternary complex. This is based on the observation that glyoxalate is buried deeper in the active site than succinate and loop closure requires succinate binding. The key step in the reaction is the deprotonation from the C^{α} atom of the carboxylate of succinate to a base, most probably by Cys 191 in the case of isocitrate lyase and Cys 123 (PrpB numbering) in the case of 2-methylisocitrate lyase. A general acid, probably Glu 295 (isocitrate lyase numbering), protonates the carboxylate adjacent to the bond formed. It has been proposed that the negative charge on the aldehyde oxygen atom of glyoxalate is stabilized by Mg^{2+} and two other basic residues [12]. In agreement with these observations, negative charge of pyruvate is stabilized by Mg^{2+} in the case of pyruvate bound PrpB model.

According to Sharma et al. [12], binding of succinate appears to trigger the movement of the Mg^{2+} by 2.5 Å towards glyoxalate, allowing Lys in the active site to form electrostatic interactions within this region and facilitating closure of the active site loop over the bound substrates. Surprisingly, in pyruvate/Mg^{2+} bound PrpB model, even in the absence of succinate, Mg^{2+} appears to have moved by approximately 2.5 Å leading to stabilization of the negative charge of pyruvate (Fig. 5). A complete understanding of the mechanism of PrpB and its differences, if any, from that of isocitrate lyase, therefore, will require the structure of PrpB-2-methylisocitrate or PrpB–pyruvate–succinate complex with the active site loop in closed conformation.

Conclusions

Analysis of the structure of *S. typhimurium* 2-methylisocitrate lyase and its complex with pyruvate/Mg^{2+} has provided important information about the active site region involved in binding of pyruvate and metal ion in the protein. Even in the absence of succinate, Mg^{2+} seems to move towards pyruvate from its position in the *E. coli* native PrpB. In the present case, the active site loop, which includes the critical cysteine residue that acts as the base during catalysis, is completely disordered in both native as well as pyruvate/Mg^{2+} bound PrpB.

Comparison of *S. typhimurium* 2-methylisocitrate lyase with the known bacterial isocitrate lyase reveals regions within the isocitrate lyase that are not present in PrpB, the smallest member of the family. These regions mainly comprise of amino and carboxy terminal ends

as well as specific insertions within loops connecting β-strands and α-helices of the $(\alpha\beta)_8$ barrel.

Sequence comparison among all known bacterial 2-methylisocitrate lyases and isocitrate lyases shows that Phe, Leu, and Pro residues, which bind pyruvate in the case of 2-methylisocitrate lyase, and Trp, Phe, and Thr, which bind glyoxalate in the case of isocitrate lyases, are strictly conserved, which seems to confer substrate specificity in these two enzymes. Similarities and differences in the structure of substrates, the active site region, and the residues that interact with the ligands in these enzymes suggest similar reaction mechanisms in isocitrate lyases and 2-methylisocitrate lyases.

Protein Data Bank accession numbers

Coordinates of native and pyruvate/Mg^{2+} bound PrpB have been deposited in the Protein Data Bank. The Protein Data Bank access codes are 1UJQ (native PrpB structure) and 1O5Q (pyruvate/Mg^{2+} bound PrpB structure).

Acknowledgments

The intensity data were collected at the X-ray Facility for Structural Biology at the Indian Institute of Science (IISc), supported by the Department of Science and Technology (DST) and the Department of Biotechnology (DBT). We thank the staff in the X-ray laboratory, Bioinformatics Centre and Supercomputing Education and Research Center of IISc for cooperation during the course of these investigations. D.K.S. thanks CSIR, India, for financial support. Assistance of P. L. Swarnamukhi during the preparation of the manuscript is gratefully acknowledged.

References

[1] S. Textor, V.F. Wendisch, A.A. De Graaf, U. Muller, M.I. Linder, D. Linder, W. Buckel, Propionate oxidation in *Escherichia coli*: evidence for operation of a methylcitrate cycle in bacteria, Arch. Microbiol. 168 (1997) 428–436.

[2] A.R. Horswill, J.C. Escalante-Semerena, *Salmonella typhimurium* LT 2 catabolizes propionate via the .2-methylcitric acid cycle, J. Bacteriol. 181 (1999) 5615–56123.

[3] R.E. London, D.L. Allen, S.A. Gabel, E.F. DeRose, Carbon-13 nuclear magnetic resonance study of metabolism of propionate by *Escherichia coli*, J. Bacteriol. 181 (1999) 3562–3570.

[4] T. Tabuchi, N. Serizawa, H. Uchiyama, A novel pathway for the partial oxidation of propionyl-CoA to pyruvate via seven-carbon tricarboxylic acids in yeast, Agric. Biol. Chem. 38 (1974) 2571–2572.

[5] T.A. Hammelman, G.A. O'Toole, J.R. Trzebiatowski, A.W. Tsang, D. Rank, J.C. Escalante-Semerena, Identification of a new prp locus required for propionate catabolism in *Salmonella typhimurium* LT2, FEMS Microbiol. Lett. 137 (1996) 233–239.

[6] A.R. Horswill, J.C. Escalante-Semerena, Propionate catabolism in *Salmonella typhimurium* LT2: two divergently transcribed units comprise the prp locus at 8.5 centisomes, prpR encodes a member of the sigma-54 family of activators, and the prpBCDE genes constitute an operon, J. Bacteriol. 179 (1997) 928–940.

[7] A.R. Horswill, J.C. Escalante-Semerena, In vitro conversion of propionate to pyruvate by *Salmonella enterica* enzymes: 2-methylcitrate dehydratase (PrpD) and aconitase enzymes catalyze the conversion of 2-methylcitrate to 2-methylisocitrate, Biochemistry 40 (2001) 4703–4713.

[8] M. Brock, R. Fischer, D. Linder, W. Buckel, Methylcitrate synthase from *Aspergillus nidulans*: implications for propionate as an antifungal agent, Mol. Microbiol. 35 (2000) 961–973.

[9] A.R. Horswill, A.R. Dudding, J.C. Escalante-Semerena, Studies of propionate toxicity in *Salmonella enterica* identify 2-methylcitrate as a potent inhibitor of cell growth, J. Biol. Chem. 276 (2001) 19094–19101.

[10] C. Grimm, A. Evers, M. Brock, C. Maerker, G. Klebe, W. Buckel, K. Reuter, Crystal structure of 2-methylisocitrate lyase (PrpB) from *Escherichia coli* and modelling of its ligand bound active centre, J. Mol. Biol. 328 (2003) 609–621.

[11] D.K. Simanshu, P.S. Satheshkumar, S. Parthasarathy, H.S. Savithri, M.R. Murthy, Cloning, expression, purification and preliminary X-ray crystallographic studies of 2-methylisocitrate lyase from *Salmonella typhimurium*, Acta Crystallogr. D 58 (2002) 2159–2161.

[12] V. Sharma, S. Sharma, K. Hoener zu Bentrup, J.D. McKinney, D.G. Russel, W.R. Jacobs Jr., J.C. Sacchettini, Structure of isocitrate lyase, a persistence factor of *Mycobacterium tuberculosis*, Nat. Struct. Biol. 7 (2000) 663–668.

[13] Z. Otwinowsky, W. Minor, Processing of X-ray diffraction data collected in oscillation mode, in: C.W. Carter Jr., R.M. Sweet (Eds.), Macromolecular Crystallography, Part A, Methods of Enzymology, vol. 276, Academic Press, New York, 1997, pp. 307–326.

[14] K. Diederichs, P.A. Karplus, Improved *R*-factors for diffraction data analysis in macromolecular crystallography, Nat. Struct. Biol. 4 (1997) 269–275.

[15] K. Huang, Z. Li, Y. Jia, D. Dunaway-Mariano, O. Herzberg, Helix swapping between two α/β barrels: crystal structure of phosphoenolpyruvate mutase with bound Mg^{2+}-oxalate, Structure 7 (1999) 539–548.

[16] J. Navaza, AMoRe: an automated package for molecular replacement, Acta Crystallogr. A 50 (1994) 157–163.

[17] A.T. Brünger, P.D. Adams, G.M. Clore, W. DeLano, P. Gros, R.W. Grosse-Kunstleve, et al., Crystallography and NMR system: a new software suite for macromolecular structure determination, Acta Crystallogr. D 54 (1998) 905–921.

[18] T.A. Jones, M. Kjeldgaard, Electron density map interpretation, Methods Enzymol. 277 (1997) 173–208.

[19] R.A. Laskowski, M.W. McArthur, D.S. Moss, J.M. Thornton, PROCHECK: a program to check the stereochemical quality of protein structures, J. Appl. Crystallogr. 26 (1993) 283–291.

[20] Collaborative Computational Project, Number 4, The CCP4 suite: programs for protein crystallography, Acta Crystallogr. D 50 (1994) 760–763.

[21] G.E. Cohen, ALIGN: a program to superimpose protein coordinates, accounting for insertions and deletions, J. Appl. Crystallogr. 30 (1997) 1160–1161.

[22] K.L. Britton, I.S. Abeysinghe, P.J. Baker, V. Barynin, P. Diehl, S.J. Langridge, et al., The structure and domain organization of *Escherichia coli* isocitrate lyase, Acta Crystallogr. D 57 (2001) 1209–1218.

[23] K.L. Britton, S.J. Langridge, P.J. Baker, K. Weeradechapon, S.E. Sedelnikova, J.R. De Lucas, et al., The crystal structure and active site location of isocitrate lyase from the fungus *Aspergillus nidulans*, Structure 8 (2000) 349–362.

[24] M. Brock, D. Darley, S. Textor, W. Buckel, 2-Methylisocitrate lyases from the bacterium *Escherichia coli* and the filamentous fungus *Aspergillus nidulans*—characterization and comparison of both enzymes, Eur. J. Biochem. 268 (2001) 3577–3586.

[25] T.L. Grimek, H. Holden, I. Rayment, J.C. Escalante-Semerena, Residues C123 and D58 of the 2-methylisocitrate lyase (PrpB) enzyme of *Salmonella enterica* are essential for catalysis, J. Bacteriol. 185 (2003) 4837–4843.

[26] M.A. Luttik, P. Kotter, F.A. Salomons, I.J. van der Klei, J.P. van Dijken, J.T. Pronk, The *Saccharomyces cerevisiae* ICL2 gene encodes a mitochondrial 2-methylisocitrate lyase involved in propionyl-coenzyme A metabolism, J. Bacteriol. 182 (2000) 7007–7013.

[27] T. Hidaka, O. Hara, S. Imai, H. Anzai, T. Murakami, K. Nagaoka, H. Seto, Biochemical mechanisms of C–P bond formation of bialaphos: use of gene manipulation for the analysis of the C–P bond formation step, Agric. Biol. Chem. 54 (1990) 2121–2125.

[28] P.J. Kraulis, MOLSCRIPT: a program to produce both detailed and schematic plots of protein structures, J. Appl. Crystallogr. 24 (1991) 946–950.

[29] E.A. Merrit, D.J. Bacon, Raster3D: photorealistic molecular graphics, Methods Enzymol. 277 (1997) 505–524.

[30] R. Esnouf, An extensively modified version of MolScript that includes greatly enhanced coloring capabilities, J. Mol. Graph. 15 (1997) 132–134.